

HIGH PERFORMNACE CONTROL OF PERMANENT MAGNET SYNCHRONOUS MOTOR UNDER DIFFERENT MODES OF OPERATION

Ibrahim M. Abdelaziz, Yehia Sayed Mohamed, Ahmed A. Zaki Diab, and E. G. Shehata,

Electrical Engineering Department, Faculty of Engineering, Minya University, Minya, Egypt ,

*Corresponding author(s) E-mail :emagameil@mu.edu.eg

Abstract

Electric vehicles (EVs) are an environmental solution providing no harmful gases with low noise. High performance EV systems require high energy-efficiency traction motors such as permanent magnet synchronous motors (PMSMs). PMSMs according to its relative advantages are commonly used for high-performance EV drive systems. PMSMs have merits of high power-to-weight ratio, high torque per ampere ratio and high efficiency. For high performance EV system, the field-oriented control (FOC) based on PI-controllers is used with a lot of hardness such as the PI-controller tuning and operating constraints. Model predictive control (MPC) can overcome such problems in FOC. In this paper, FOC and finite-set model predictive control (FS-MPC) techniques for an interior permanent magnet synchronous motor (IPMSM) are analyzed under different operating modes. For EV applications, IPMSMs are operated under maximum torque per ampere (MTPA) and field weakening (FW) operating modes. FS-MPC depends on the on-line solution of a Quadratic programming (QP) problem cost function to overcome problems of the cascaded structure of PI-controllers loops in FOC. The performance of the proposed two controllers is compared under the same operating conditions. Simulation results show that the proposed FS-MPC technique enhances the performances compared with the common ordinary cascaded structure FOC.

Keywords: *Electric Vechicle, IPMSM control,FOC, FC-MPC , MTPA, Field-Weakening region.*

1. Introduction

Electric Vehicles has a wide applicable field of the electrical drives and clean energy enhancement. EVs are environmental (no harmful gases and low noise) and unbinding for the city traffic. Nowadays, electric vehicles can replace traditional vehicles which use internal combustion engines (ICEs). EV is facing the soaring prices of fossil fuel, reducing the carbon emission, and becoming an environment friendly technology [1]. The machine type and its characteristics form the essential factor for any EV model's success [2]. High-performance EV systems require a high energy-efficiency traction motor so that PMSM is used for this paper. PMSMs have merits such as no rotor copper loss leading to

high efficiency, high torque per inertia ratio, and high power-to-weight ratio [2-3]. PMSM may be surface mounted type (SM-PMSM) or interior type according to the configuration of the permanent magnet in the rotor. Permanent magnet synchronous rotor became more popular for EV drives system for low and medium power range up to 10 kW and nowadays PMSM used up to 30 kW [3-6]. A Comprehensive study on PMSMs drive Systems for various electrical transportation applications is presented [3]. In [4], a radial flux inner-rotor PMSM is designed to achieve EV requirements. A general overview of electric machines for electric and hybrid vehicles is presented in [5,7]. In [6], a PMSM is design using high energy neodymium-iron-boron (Nd-Fe-B) permanent magnet material

to satisfy the special requirements of, high-power density, high- efficiency, high starting-torque, and high cruising speed for EVs. A novel study for brushless motor drives is developed in [8]. In [9], a performance fuzzy PI speed controller is designed comparing to the sliding mode control. In [10], a novel scheme is proposed to reduce the problems of systems fed by multi-level inverters such as computational complexity and high switching loss for space vector-pulse width modulation (SV-PWM) for PMSM-FOC and verified results by simulation and experimentally. Direct torque control operation via a wide speed range is proposed in [11] based on the torque and stator linkage flux control. A Look-Up table (LUT) for MTPA and a reverse relation between the speed and the voltage vector during FW are applied. In [12], an integral FS-MPC based on linearizing of the SM-PMSM state space model is proposed resulting in zero steady state error with load torque disturbance rejection. In [13], a MPC for PMSM including the FW for SM-PMSM is presented by linearizing the machine model verifying by simulation and experiment. In [14], a compensated MPC with Simplified Repetitive Control proposed to improve the MPC robustness against current distortion, parameter mismatch and dead time effect for SM-PMSM drives. This paper presents and implements a MPC technique compared to the conventional FOC based on PI-controller by using MATLAB-Simulink. The paper is organized as following: PMSM dynamic model is introduced in Section 2. Section 3 introduces modes of operation of a PMSM. Section 4 introduce PMSM control FOC and the proposed MPC. Simulation results are given in Section 5. Finally, a conclusion is given in Section 6.

2. IPMSM Model

Electrical model of the IPMSM in the d-q reference frame is:

$$u_{ds} = R_s i_{ds} + L_{ds} \frac{di_{ds}}{dt} - \omega_m L_{qs} i_{qs} \quad (1)$$

$$u_{qs} = R_s i_{qs} + L_{qs} \frac{di_{qs}}{dt} + \omega_m L_{ds} i_{ds} + \omega_m \phi_f \quad (2)$$

$$J \frac{d\Omega_m}{dt} = T_{em} - T_l \quad (3)$$

$$\frac{d\omega_m}{dt} = \frac{Z_p}{J} (T_{em} - T_l) \quad (4)$$

$$T_{em} = \frac{3Z_p}{2} (\phi_f i_{qs} + (L_{ds} - L_{qs}) i_{ds} i_{qs}) \quad (5)$$

$u_{ds}, u_{qs}, i_{ds}, i_{qs}$: the d-q stator voltages and currents respectively.

R_s : the stator winding resistance in ohm.

J : the moment of inertia in kg.m².

ϕ_f : the permanent magnet rotor flux.

L_{ds}, L_{qs} : the stator d-q axis inductances in Henry.

T_l : the load torque that is considered as unknown disturbance.

ω_m : the electrical motor speed in electrical rad/s that equal the rotor mechanical speed (Ω_m) multiplied by the pole pairs (Z_p) as in Eq.6

$$\omega_m = Z_p \Omega_m \quad (6)$$

T_{em} : the electromagnetic torque consists of two terms; the first term is the magnetic torque produced by the PM. Flux and the second term is the reluctance torque produced by the difference between the d-q reluctances according to the interior permanent magnet motor d-q axes reluctance design.

3. Operating Modes of PMSMs

Between the different operating modes of PMSMs such as constant torque angle [12], unity power factor [15] and maximum efficiency [16] operations there are two common operating regions, constant torque and field weakening operating modes [11].

3.1 Constant torque angle control technique

Constant torque angle control is achieved by maintain the angle between the stator phasor current i_s and the rotor d-axis flux to be 90°, which means i_{ds} equals zero as shown in Fig.1. This mode is used for energy saving during steady

state operation and is suitable for SM-PMSM. If this mode of operation is applied to IPMSM, reluctance torque will be disappeared which decrease the motor efficiency.

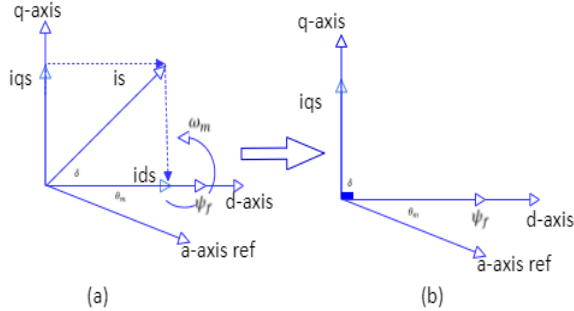


Fig.1 Constant torque angle operation vector diagram.

3.2 Optimized torque per ampere control technique.

According to Eq.5 to get positive reluctance torque for IPMSM ($L_{ds} > L_{qs}$), i_{ds} must be negative value. From Fig.2 we get:

$$i_s = \sqrt{i_{ds}^2 + i_{qs}^2} \quad (6)$$

$$i_{qs} = i_s \sin(\delta) \quad (7)$$

$$i_{ds} = i_s \cos(\delta) \quad (8)$$

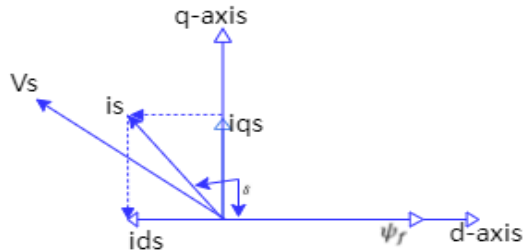


Fig.2 vector diagram for stator currents.

By substituting Eq.7&8 into Eq.5 to get the d-axis current corresponding to command torque:

$$i_{ds}^{cmd} = \frac{\phi_f}{2(L_{qs} - L_{ds})} - \sqrt{\left(\frac{\phi_f}{2(L_{qs} - L_{ds})}\right)^2 + i_{qs}^2} \quad (9)$$

By substituting in Eq.5, a relation between torque and command i_{qs}^{cmd} is obtained as:

$$T_{em}^{cmd} = \frac{3 Z_p}{2} i_{qs} \left[\frac{\phi_f}{2} + \sqrt{\left(\frac{\phi_f}{2}\right)^2 + ((L_{qs} - L_{ds})i_{qs})^2} \right] \quad (10)$$

Using Eq.10 and known values of torque, the corresponding q-axis current could be calculated. Putting these values in a lookup table to calculate the command q-axis current for different command torques. Finally, the command d-q axes current required for the inner loop calculated by using Eq.9 and the lookup table.

3.3 Field weakening operation

At steady state operation the machine model is:

$$u_{ds} = R_s i_{ds} - \omega_m L_{qs} I_{qs} \quad (11)$$

$$u_{qs} = R_s I_{qs} + \omega_m L_{ds} I_{ds} + \omega_m \phi_f \quad (12)$$

$$\phi_s = \sqrt{\phi_{ds}^2 + \phi_{qs}^2} \quad (13)$$

$$\phi_{ds} = L_{ds} I_{ds} + \phi_f \quad (14)$$

$$\phi_{qs} = L_{qs} I_{qs} \quad (15)$$

$$u_s = \sqrt{u_{ds}^2 + u_{qs}^2} = \omega_m \sqrt{\phi_{ds}^2 + \phi_{qs}^2} \quad (16)$$

$$emf_{ds} = \omega_m L_{ds} I_{ds} + \omega_m \phi_f \quad (17)$$

$$emf_{qs} = \omega_m L_{qs} I_{qs} \quad (18)$$

where: emf_{ds}, emf_{qs} : the stator d-q induced electromotive force that proportional to the motor speed times the stator axes flux known as cross coupling terms. To get higher motor speed without the machine saturation we reduce the flux that is known Field Weakening. The FW technique requires high negative d-axis current and reduced q-axis current to get the maximum torque required during the FW operation. For the critical constrained point (neglecting stator resistance):

$$\left(\frac{u_{smax}}{\omega_m}\right)^2 = (L_{ds} i_{ds} + \phi_f)^2 + (L_{qs})^2 (I_{smax}^2 - i_{ds}^2) \quad (19)$$

Then,

$$(L_{ds}^2 - L_{qs}^2) i_{ds}^2 + 2L_{ds} \phi_f i_{ds} + (\phi_f^2 + L_{qs}^2 I_{smax}^2) - \left(\frac{u_{smax}}{\omega_m}\right)^2 = 0 \quad (20)$$

For a required speed, Eq.20 is a quadratic Eq. for d-axis current that is solved to give the command d-axis current as:

$$i_{ds}^{cmd} = \frac{-2L_{ds}\theta_f + \sqrt{(2L_{ds}\theta_f)^2 - 4(L_{ds}^2 - L_{qs}^2)(\theta_f^2 + L_{qs}^2 I_{s,max}^2) - \left(\frac{U_{s,max}}{\omega_m}\right)^2}}{2(L_{ds}^2 - L_{qs}^2)} \quad (21)$$

Then, by using Eq.6 we get the command q-axis current as:

$$i_{qs}^{cmd} = \sqrt{I_{s,max}^2 + (i_{ds}^{cmd})^2} \quad (22)$$

Using the command d-q currents, the maximum torque is calculated and then compared to the command from the PI speed controller. The smaller value is chosen according to Eq.23&24 [17]. Then update the q-axis current from the selected torque value via Eq.5.

$$T_{em}^{max} > T_{em}^{cmd} \rightarrow T_{em} = T_{em}^{cmd} \quad (23)$$

$$T_{em}^{max} < T_{em}^{cmd} \rightarrow T_{em} = T_{em}^{max} \quad (24)$$

4. FOC and MPC of PMSM

4.1 Field Oriented Control for PMSM

Figure 3 shows the schematic diagram of the field-oriented control. FOC technique consists of two cascaded control loops with three PI-controllers. The outer loop for speed regulation that produce the reference currents required for the inner control loops according to the operation mode. The inner d-q axis controllers regulate v_{ds} & v_{qs} terms. The emf compensated terms are added to enhance the performance during steady state operation as shown in Fig.4. Without compensating terms, stator voltage in synchronous frame can be expressed as:

$$v_{ds} = R_s i_{ds} + L_{ds} \frac{di_{ds}}{dt} \quad (25)$$

$$v_{qs} = R_s i_{qs} + L_{qs} \frac{di_{qs}}{dt} \quad (26)$$

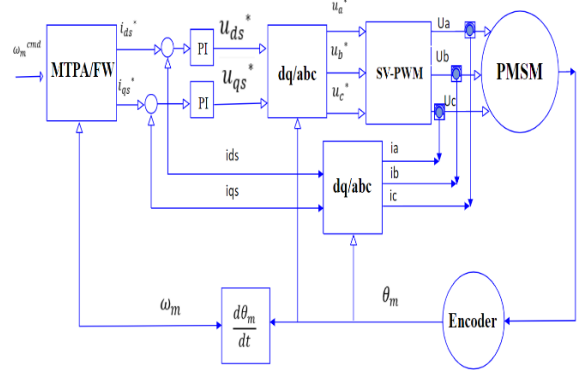


Fig.3 schematic diagram of FOC for PMSM.

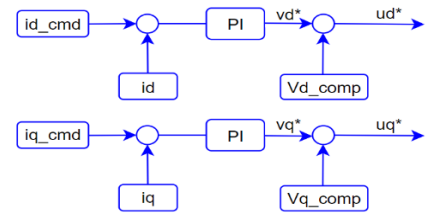


Fig.4 Inner control loops schematic diagram

In s-domain the steady state d-q axis transfer function of PMSM and the PI controller are:

$$\frac{i_{ds}(s)}{v_{ds}(s)} = \frac{1/L_{ds}}{s + R_s/L_{ds}} \quad (27)$$

$$\frac{i_{qs}(s)}{v_{qs}(s)} = \frac{1/L_{qs}}{s + R_s/L_{qs}} \quad (28)$$

$$PI(s) = K_p + \frac{K_i}{s} \quad (29)$$

Where: K_p and K_i are the proportional and the integral gains of the PI-controller. For PI-controller design, neglecting the compensation terms and considering the transfer function of the inverter is 1, result the simplified control loops are shown in Fig.5. Comparing the second order inner closed loop transfer function to the standard form in Eq.29 with damping ratio $\zeta = 0.707$ and natural undamped natural frequency $\omega_{inner} = 100 \text{ rad/s}$, gives the inner loops' PI-controller gains.

$$TF = \frac{\omega_n^2}{s^2 + 2\zeta\omega_n s + \omega_n^2} \quad (30)$$

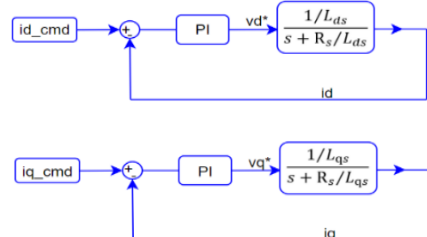


Fig.5 Simplified d-q axis current loops

The simplified speed loop transfer function is:

$$\frac{\omega_m(s)}{i_{qs}(s)} \approx \frac{\frac{3Z_p^2 \phi_f}{2J}}{s + \frac{B}{J}} \quad (31)$$

With $\zeta = 1$ and slower frequency $\omega_{out} = 0.1\omega_{inner}$ rad/s, PI-controller gains can be designed for outer loop. The performance of the system with these gains is still not good. After all, for more effective performance gains are tuned by MATLAB. Finally, the compensated terms are added to get the command d-q axis voltages. The command stator voltages are limited by the amplitude of the space vector voltage signal that equals $1/\sqrt{3}$ times the DC-Link voltage for Space Vector Pulse Width Modulation (SV-PWM). The d-q voltages limits are identified by the constraints as shown in Fig 6.

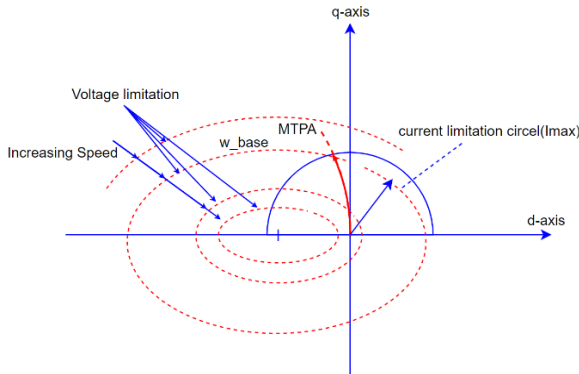


Fig.6 Constraints for d-q axes voltage and current

The d-q axis maximum command voltages [18] in the following Equations.

$$\sqrt{v_{ds}^2 + v_{qs}^2} = \frac{V_{dc}}{\sqrt{3}} \quad (32)$$

$$v_{qs_max}^* = \epsilon \frac{V_{dc}}{\sqrt{3}} \quad (33)$$

$$v_{ds_max}^* = \sqrt{1 - \epsilon^2} \frac{V_{dc}}{\sqrt{3}} \quad (34)$$

The d-q axis rotating reference frame command voltages are transformed to the three-phase reference frame and then applied to the SV-PWM algorithm.

4.2 Finite Set-Model Predictive Control for PMSM Drives

In recent years, MPC becomes commonly applicable for applications of electric drives and power electronics because of the fast development in micro-controllers and advances in MPC research and its advantages such as [19,20]:

- Concepts are very easy to understand.
- The multivariable case can be easily considered.
- Easy inclusion of non-linearities in the model, without the need to linearize the model for a given operating point and improving the operation of the system for all conditions.
- Using predictive control, it is possible to avoid the cascaded structure, used in a linear control scheme, obtaining very fast transient responses.
- The MPC controller is easy to be implemented.

The proposed MPC control for PMSM drive consists of two steps. The outer loop uses a PI-controller to regulate the speed by producing the command torque. The d-q axes command currents are calculated according to the operating regions of the PMSM, MTPA/FW required as set points for the inner loop MPC current regulation. The inner control MPC algorithm based on [20]:

- Using a model to predict the future behavior of the variables in a horizon time.
- A cost function representing the desired system behavior.
- The optimal control action is obtained by minimizing the cost function.

In another words, there are eight voltage vectors of the inverter switching cases as in matrix U. MPC applies the eight switching cases on the PMSM model to predict the next step current vector i_k as in Eq.35. Based on

the instant command current vector, measured currents and the rotor speed and its position, the predicted current vector is calculated as:

$$i_k = F * i + G * M * D * U(:, k) + H \quad (35)$$

where:

$$i_k = [i_{ds}(t_{i+1}); i_{qs}(t_{i+1})], i = [i_{ds}(t_i); i_{qs}(t_i)]$$

$$F = \begin{bmatrix} 1 - \frac{R_s T_s}{L_{ds}} & \frac{\omega_m L_{qs} T_s}{L_{ds}} \\ \frac{\omega_m L_{ds} T_s}{L_{qs}} & 1 - \frac{R_s T_s}{L_{qs}} \end{bmatrix}, G = \begin{bmatrix} T_s & 0 \\ 0 & T_s \end{bmatrix}$$

$$H = \begin{bmatrix} 0 \\ -\frac{\omega_m \phi_f T_s}{L_{qs}} \end{bmatrix}, M = \begin{bmatrix} \cos(\theta_m) & \sin(\theta_m) \\ -\sin(\theta_m) & \cos(\theta_m) \end{bmatrix}$$

$$D = \frac{2}{3} V_{dc} \begin{bmatrix} 1 & -0.5 & -0.5 \\ 0 & \frac{\sqrt{3}}{2} & -\frac{\sqrt{3}}{2} \end{bmatrix}, \theta_m = \int \omega_m dt$$

$$U = \begin{bmatrix} 0 & 1 & 1 & 0 & 0 & 0 & 1 & 1 \\ 0 & 0 & 1 & 1 & 1 & 0 & 0 & 1 \\ 0 & 0 & 0 & 0 & 1 & 1 & 1 & 1 \end{bmatrix}$$

The predicted current vector is applied to a quadratic error problem between the command current and the predicted values. An optimal loop algorithm is applied to select the more suitable vector to minimize the quadratic cost function in Eq.36 [19].

$$g = (i_{ds}^*(t_i) - i_{ds}(t_{i+1}))^2 + (i_{qs}^*(t_i) - i_{qs}(t_{i+1}))^2 \quad (36)$$

where $i_{ds}^*(t_i)$, $i_{qs}^*(t_i)$ are the command d-q axis current at time instant of t_i and $i_{ds}(t_{i+1})$, $i_{qs}(t_{i+1})$ are the predicted d-q axis currents for the next time step t_{i+1} . Finally for every control step time (10^{-4} s) we get the optimized switching cases for the inverter switches required to produce this optimal voltage vector and apply it to the inverter directly without need for another step of PWM as in vector control. We use the measured speed by the encoder and rotor position to get the actual d-q currents from the measured three phase

values by Clark transformation and then the direct rotational transformation matrix. The MPC schematic diagram is shown in Fig.7, and the machine parameters are illustrated in Table 1.

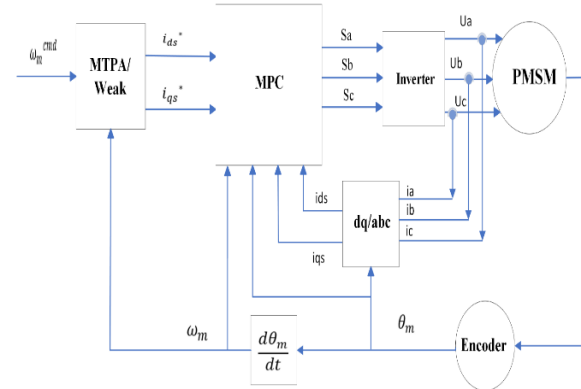


Fig.7 FC-MPC schematic control for PMSM drive

Table 1 The PMSM parameters.

Symbol	Description	Value
Z_p	Pole Paris	2
J	Moment of inertia	0.021 kg.m ²
B	Viscous friction	≈ 0
R_s	Stator resistance	1.4852 Ω
L_{ds}	d-axis stator inductance	0.0955 H
L_{qs}	q-axis stator inductance	0.1415 H
ϕ_f	Rotor PM flux	0.3847
ω_m	Rated speed	2000 rpm
T_{em}	Rated electro-magnetic torque	7.162 Nm
V_{dc}	DC-Link voltage	540 V
I_s	Phase current amplitude	7.4 A
P	Rated power	1.5 kW

5. Simulation Results and discussion

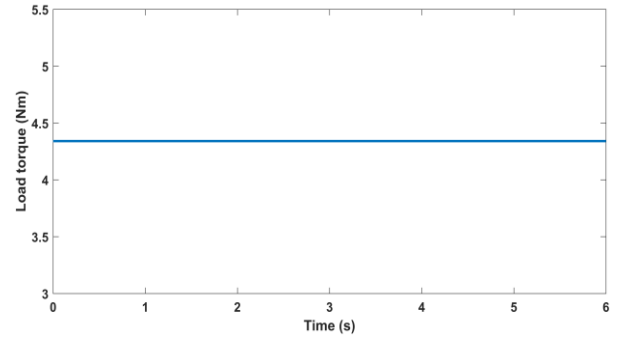
The proposed FOC/MPC control techniques incorporating both the MTPA/FW controllers are modeled and simulated by MATLAB-Simulink for IPMSM of Table 1. For FOC PWM a three-phase inverter model based on insulated gate bipolar transistors (IGBTs) which is supplied with a dc-link voltage of 540 V. The PWM frequency of the

inverter is set at 4.050 kHz ($=3 \times 27 \times 50$, odd multiple of 3 times the frequency to illuminate the third harmonic and its multipliers) and for control is 10 kHz as usual for two-level IGBT-based inverters sample time. The PMSM characteristics are discussed under fixed load torque as in case 1, and under changeable load disturbance as in case 2. The PI-controller used for speed regulation with FOC and FC-MPC is the same.

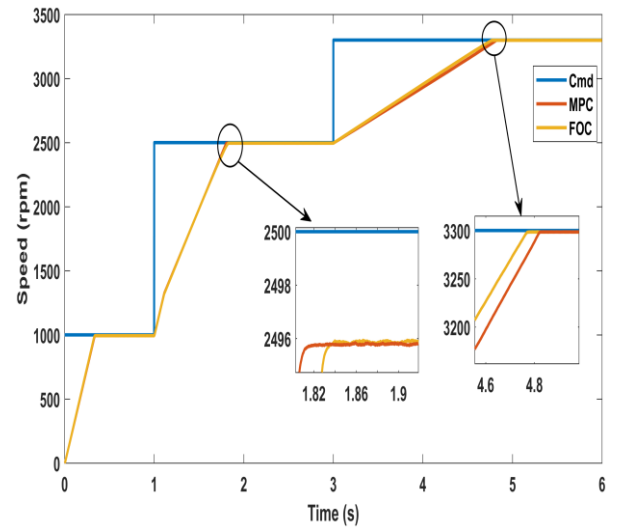
Case (1): Variable motor speed with fixed load torque.

The motor speed is changed from 1000 rpm to 3000 rpm then for 3300 rpm. The load torque is fixed at rated value of 4.3406 Nm for 3300 rpm speed. The simulation results are given in Fig.8. Results show, the motor speed waveforms of the two techniques are identical. The command torque follows the maximum allowable as a function of the speed. The power trajectory is maintained at its maximum limit during the field-weakening operation. The drive speed is smoothly reached the command during all the operation. MPC has better dynamic performances than for FOC due to d-q axis voltages saturation in FOC. This voltage saturation causes a sudden magnitude reduction in torque and so the d-axis current that is not existing in MPC. The d-q axis MPC/FOC currents follow the command within the inverter limits with more precisely for MPC. MPC currents have lower ripple during the dynamic and steady state operation. MPC three phase currents have lower harmonic distortion than in FOC as in Fig.8 (e and f). During high-speed FW operation with the rated power 1500 W, MPC has better steady state performance with lower ripple in torque and currents waveforms. The lower current ripple for MPC can

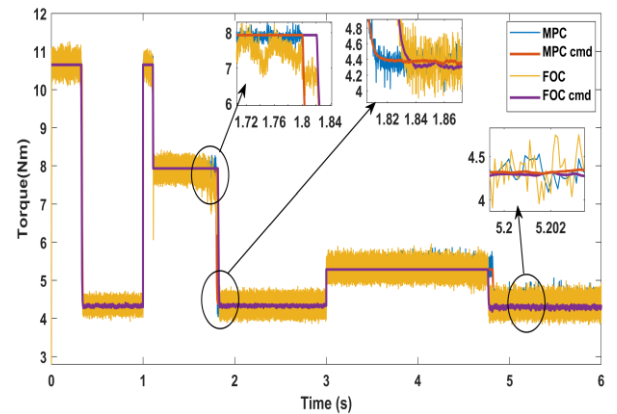
extend a wider speed bandwidth. Independent of the control technique, the PMSM has better performance for lower speed than for the high speed, because of high inductances and permanent magnet flux.



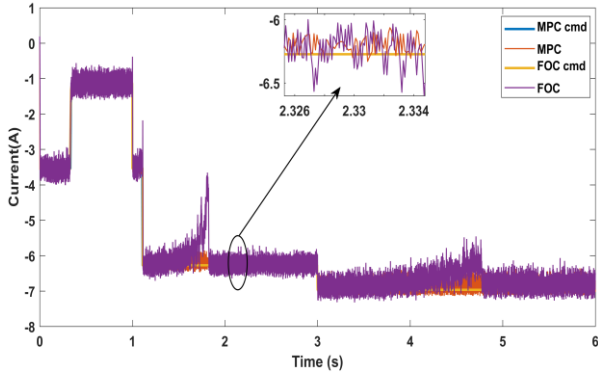
(a) Load torque



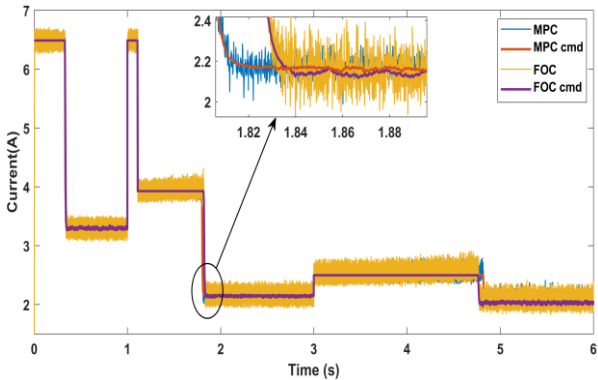
(b) Reference and actual motor speed.



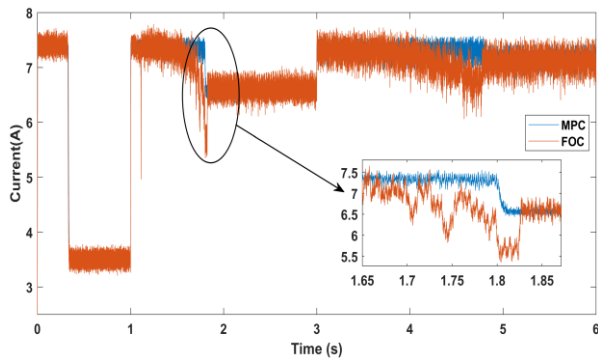
(c) Electromagnetic torque.



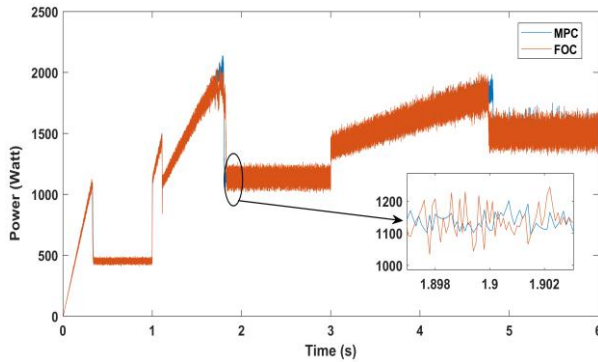
(d) d-axis stator current.



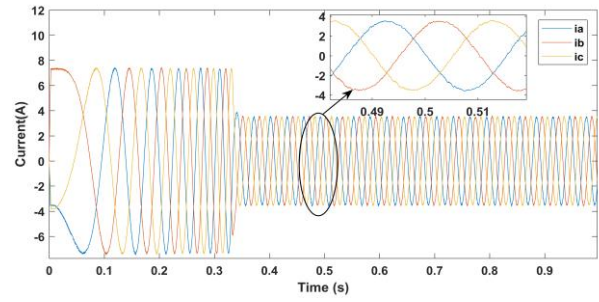
(e) q-axis stator current



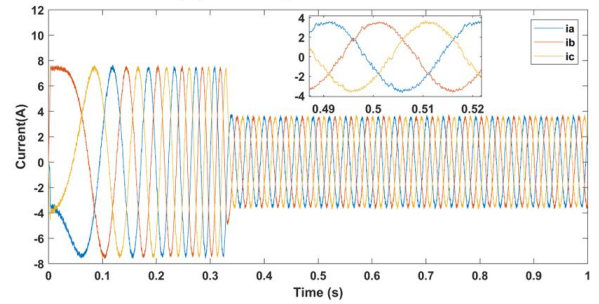
(c) Stator current amplitude



(d) Motor output power



(e) Three phase MPC current

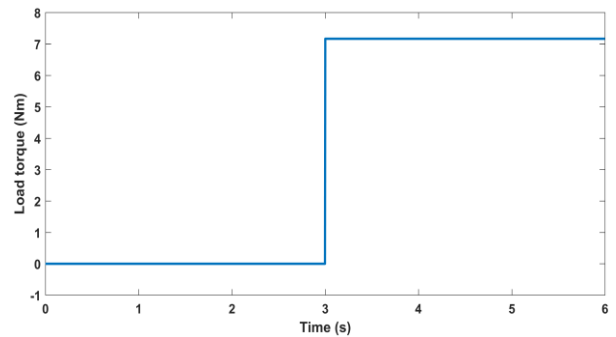


(f) Three phase FOC current

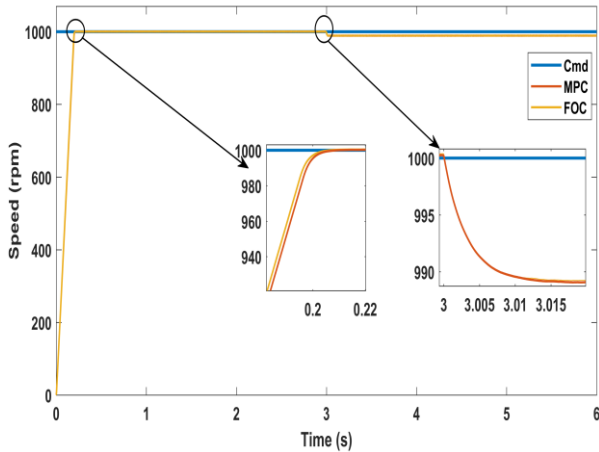
Fig.8 Under constant load torque results Validation. (a) T_l (b) ω_m , (c) T_{em} , (d) i_{ds} , (e) i_{qs} , (f) i_s , (g) P , (h) i_{abcMPC} , and (i) i_{abcFOC}

Case 2: Variable load torque.

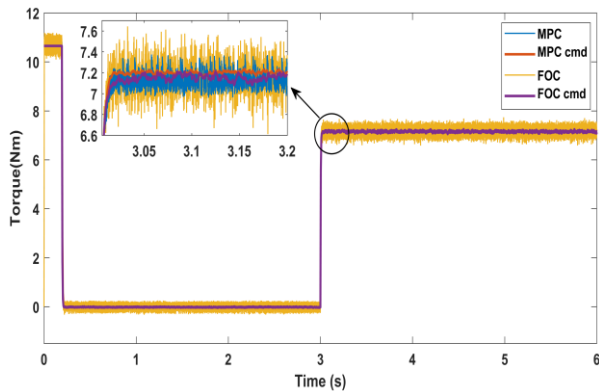
Figure 9 shows waveforms of the MPC/FOC under sudden rated load torque (7.162 Nm) impose at 3s. The operation is during MTPA control region at rated speed of 1000 rpm. The motor speed is constant and equal to the command with just 1% drop. MPC/FOC speed response are identical. It is observed that the MPC has a lower torque and current ripple with sudden load impose.



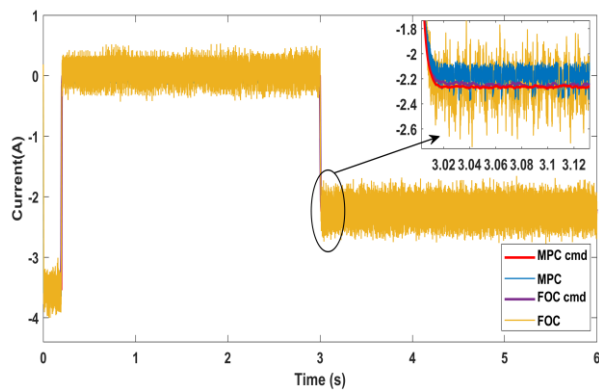
(a) Load torque variation



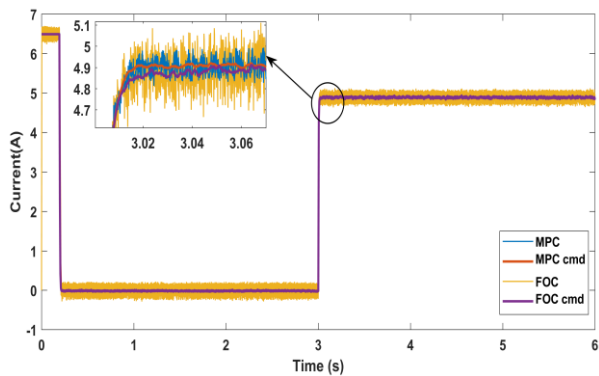
(b) Motor speed.



(c) Electromagnetic torque



(d) d-axis current



(e) q-axis current

Fig.9 Variable Load Torque results Validation.(a) T_l , (b) ω_m , (c) T_{em} , (d) i_{ds} , and (e) i_{qs}

6. Conclusion

Two controllers FOC and FS-MPC scheme for IPMSM drives are proposed and implemented. IPMSM operated at MTPA and FW under constant load and sudden load torque impose. Within the inverter's limit of current and voltage, MTPA/FW is implemented. Simulation results show that MPC has better performance over the whole MTPA/FW dynamic and steady state operation. MPC presents some benefits over FOC control such as easier control reduced ripple and harmonics, the torque and currents waveform follow the command precisely than for FOC, and so there is no gain tuning problem. MPC is a high computational technique that does not still a problem with the advance in controllers and MPC research.

REFERENCES

- [1] Chin, Jun-Woo, et al. "High efficiency PMSM with high slot fill factor coil for heavy-duty EV traction considering AC resistance." IEEE Transactions on Energy Conversion 36.2 (2020): 883-894.
- [2] Chin, Jun-Woo, et al. "High efficiency PMSM with high slot fill factor coil for heavy-duty EV traction considering AC resistance." IEEE Transactions on Energy Conversion 36.2 (2020): 883-894.
- [3] Chau, K. T., and Wenlong Li. "Overview of electric machines for electric and hybrid vehicles." International Journal of Vehicle Design 64.1 (2014): 46-71.
- [4] Menon, Rishi, et al. "A comprehensive survey on permanent magnet synchronous motor drive systems for electric transportation applications." IECON 2016-42nd Annual Conference of the IEEE

- Industrial Electronics Society. IEEE, 2016.
- [5] Loganayaki, A., and R. Bharani Kumar. "Permanent Magnet Synchronous Motor for Electric Vehicle Applications." 2019 5th International Conference on Advanced Computing & Communication Systems (ICACCS). IEEE, 2019.
- [6] Flah, Aymen, et al. "Field-oriented control strategy for double-stator single-rotor and double-rotor single-stator permanent magnet machine: Design and operation." *Computers & Electrical Engineering* 90 (2021): 106953.
- [7] Sun, Xiaodong, et al. "Analysis and design optimization of a permanent magnet synchronous motor for a campus patrol electric vehicle." *IEEE Transactions on Vehicular Technology* 68.11 (2019): 10535-10544.
- [8] Sheela, A., et al. "FEA based analysis and design of PMSM for electric vehicle applications using magnet software." *International Journal of Ambient Energy* (2020): 1-6.
- [9] Chen, Qiping, et al. "PMSM control for electric vehicle based on fuzzy PI." *International Journal of Electric and Hybrid Vehicles* 12.1 (2020): 75-85.
- [10] Yao, Huan, et al. "A Novel SVPWM Scheme for Field-Oriented Vector-Controlled PMSM Drive System Fed by Cascaded H-Bridge Inverter." *IEEE Transactions on Power Electronics* 36.8 (2021): 8988-9000.
- [11] Rahman, Muhammed Fazlur, L. Zhong, and Khiang Wee Lim. "A direct torque-controlled interior permanent magnet synchronous motor drive incorporating field weakening." *IEEE Transactions on Industry Applications* 34.6 (1998): 1246-1253.
- [12] Akhil, R. S., et al. "Modified flux-weakening control for electric vehicle with PMSM drive." *IFAC-PapersOnLine* 53.1 (2020): 325-331.
- [13] Chai, Shan, Liuping Wang, and Eric Rogers. "Model predictive control of a permanent magnet synchronous motor with experimental validation." *Control Engineering Practice* 21.11 (2013): 1584-1593.
- [14] Liu, Ying, et al. "Robust model predictive control with simplified repetitive control for electrical machine drives." *IEEE Transactions on Power Electronics* 34.5 (2018): 4524-4535.
- [15] Andreescu, Gheorghe-Daniel, et al. "Stable V/f control system with unity power factor for PMSM drives." 2012 13th international conference on optimization of electrical and electronic equipment (OPTIM). IEEE, 2012.
- [16] Balamurali, Aiswarya, et al. "Noninvasive and improved torque and efficiency calculation toward current advance angle determination for maximum efficiency control of PMSM." *IEEE Transactions on Transportation Electrification* 6.1 (2019): 28-40.
- [17] Mynar, Zbynek, Libor Vesely, and Pavel Vaclavek. "PMSM model predictive control with field-weakening implementation." *IEEE Transactions on Industrial Electronics* 63.8 (2016): 5156-5166.
- [18] Krishnan, Ramu. "Control and operation of PM synchronous motor drives in the field-weakening region." *Proceedings of IECON'93-19th Annual Conference of IEEE Industrial Electronics*. IEEE, 1993.
- [19] Wang, Liuping, et al. *PID and predictive control of electrical drives and power converters using MATLAB/Simulink*. John Wiley & Sons, 2015.
- [20] Rodriguez, Jose, and Patricio Cortes. *Predictive control of power converters and electrical drives*. Vol. 40. John Wiley & Sons, 2012.

